



**AIAA-2000-0293**

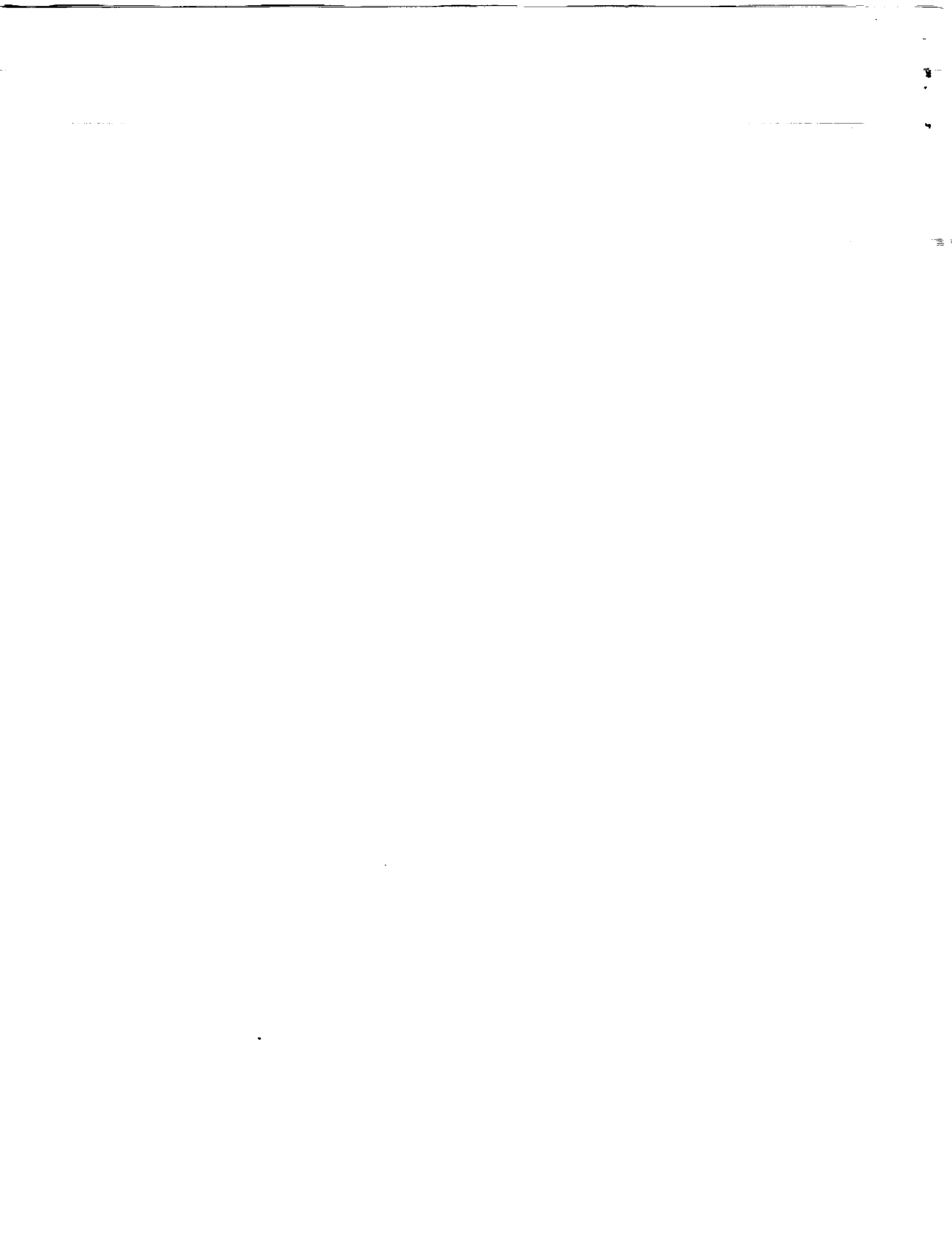
**National Transonic Facility Characterization  
Status**

C. Bobbitt, Jr., J. Everhart, J. Foster, J. Hill, R. McHatton, and  
W. Tomek

NASA Langley Research Center  
Hampton, Virginia

**38th Aerospace Sciences Meeting & Exhibit**  
10-13 January 2000  
Reno, Nevada

For permission to copy or republish, contact the American Institute of Aeronautics and Astronautics,  
1801 Alexander Bell Drive, Suite 500, Reston, Va, 20191-4344



## NATIONAL TRANSONIC FACILITY CHARACTERIZATION STATUS

C. Bobbitt, Jr., J. Everhart, J. Foster, J. Hill, R. McHatton, W. Tomek  
 NASA Langley Research Center  
 Hampton, Virginia USA

### Abstract

This paper describes the current status of the characterization of the National Transonic Facility. The background and strategy for the tunnel characterization, as well as the current status of the four main areas of the characterization (tunnel calibration, flow quality characterization, data quality assurance, and support of the implementation of wall interference corrections) are presented. The target accuracy requirements for tunnel characterization measurements are given, followed by a comparison of the measured tunnel flow quality to these requirements based on current available information. The paper concludes with a summary of which requirements are being met, what areas need improvement, and what additional information is required in follow-on characterization studies.

### National Transonic Facility (NTF) Characterization Background

#### Characterization Background

The purpose of wind-tunnel testing is to study aerodynamic phenomena in a known, controlled environment that matches a desired target flow condition. Any deviation in the flow field from this target flow results in inaccuracies in the desired measurements. This deviation can be due to the freestream

non-uniformities or unsteadiness, or adverse model/tunnel wall interactions. The amount of deviation allowable in the flow field from the target flow is governed by the required accuracy in the desired measurements. Therefore, to provide high-quality wind-tunnel data, we must determine the required accuracy in measurements; translate these requirements into requirements on the flow field; determine if the tunnel flow meets these requirements; and determine the impact and possible solutions if the flow field does not meet these requirements.

#### Facility Background

The NTF was primarily designed to achieve flight-Reynolds numbers at transonic speeds using a combination of high pressures and cryogenic temperatures. It is a closed-circuit tunnel with a single-stage compressor, a 15:1 contraction ratio, and a 25-foot long, 8.2-foot square test-section with filleted corners. The test-section can be run in a slotted-wall (top and bottom walls slotted with a 6-percent openness ratio) or a solid-wall configuration. **Figure 1** shows a layout of the tunnel, with the nitrogen injection ring between turns 1 and 2, the inlet guide vanes, fan, and stators between turns 2 and 3, and the heat exchanger and four turbulence reduction screens in the settling chamber just upstream of the contraction region. Tunnel specifications are given in **Table 1**. The tunnel can be run with either air or nitrogen as the test-medium. In

- |  |                   |
|--|-------------------|
| • Test-section area:   | 8.2 ft. x 8.2 ft  |
| • Mach range:  | 0.10 to 1.2       |
| • Pressure range (atm.):   | 1 to 9            |
| • Temperature range (F):   | -260 to 130       |
| • Max Reynolds number  | 120 million / ft. |
| (based on chord or $0.1 \cdot \sqrt{\text{test-section area}}$ ) |                   |

**Table 1 – NTF Specifications**

the air mode, temperature control is achieved using a water-filled heat exchanger; in the nitrogen mode, temperature control is achieved by the injection of liquid nitrogen into the flow. Mach number control is achieved using a combination of selected fan speed and inlet guide vane angles. The NTF can test sting-mounted full-span models and sidewall-mounted semi-span models.

#### NTF Characterization Strategy

The first step in developing the strategy for the characterization of the NTF was to create an overarching process that would result in verifiable flow quality and data quality that met customer expectations. The process created for the NTF characterization is shown as a flow chart in **Figure 2**. The first step in the process is to determine the customer accuracy requirements for aerodynamic measurements made at the NTF. These requirements are then used to compute accuracy requirements for the flow parameters using the technique of propagation of errors. Next, the flow parameters are measured in the wind-tunnel and compared to the accuracy requirements. If the requirements are met, the flow parameters must be periodically checked to insure continued compliance. If the accuracy requirements are not being met, corrective action must be taken, and measurements made to see if the flow parameters then comply with the requirements. This process is to be continued throughout the life of the wind-tunnel, with periodic review to insure measurement accuracy requirements meet current testing needs.

Accuracy requirements at the NTF are driven by performance testing, and are most stringent for measurement of lift and drag coefficients. Input was obtained from several industry

customers who frequently test at the NTF to determine what accuracy is being sought for these aerodynamic measurements. These requirements are shown in **Table 2**. Subsequently, all characterization efforts have been focused on meeting these requirements.

The NTF characterization effort consists of four main areas: tunnel calibration; flow quality characterization; data quality assurance; and support of the implementation of wall interference corrections. The calibration and flow quality areas focus on the short-term accuracy of individual flow parameters throughout the test-section over the operating range of the tunnel. The data quality assurance thrust is designed to provide accuracy of calibration parameters and force coefficients both short-term and long-term, and to insure that the tunnel measurements remain stable. The support of the implementation of wall interference corrections provides information critical for correcting biases in the aerodynamic measurements due to model/tunnel wall interactions.

Two novel ideas were incorporated in the NTF characterization strategy. The first was to divide the test segments into short-duration, self-contained tests. This approach allows the ability to fit characterization tests into small windows of opportunity, which results in minimum impact to the tunnel schedule. Additionally, this strategy allows time for lessons learned in one characterization test segment to be implemented in any following test. The second idea was to publish and present all characterization data as soon as possible. This openness of communication allows customers testing at the NTF to better understand their data, and encourages customer feedback with input and insight into

#### High-lift

- 0.4%  $C_L$ ,  $C_D$  absolute
- 0.2%  $C_L$ ,  $C_D$  incremental

#### Transonic cruise

- 1 count  $C_D$  absolute
- 1/2 count  $C_D$  incremental

**Table 2 – Customer Accuracy Requirements**

possible causes and corrections if the flow quality does not meet the accuracy requirements in a certain area.

The remainder of this paper provides the status of the four areas of the NTF characterization.

### Calibration and Empty Tunnel Flow Quality

#### Flow Quality Requirements

Much work has been done in previous efforts to determine accuracy requirements for wind-tunnel measurements and translate these into requirements for the wind-tunnel flow. Most notably, a recent in-depth analysis of flow quality requirements was completed and documented by the National Wind Tunnel Complex (NWTC) Project team consisting of members from the U.S. government, industry and academia. These NWTC Project requirements were determined to be the best approximation of an agreed-upon national standard for wind-tunnel flow quality, and were therefore adopted as goals for this flow quality characterization effort. **Table 3**, taken from the NWTC documentation (Binion/Steinle<sup>1</sup>), provides a summary of the parameters defining the flow field and accuracy requirements for both low-speed and transonic testing.

#### Temperature Characterization

Temperature measurements have been made at the NTF using a thermocouple grid located in the settling chamber between the cooling coil and the most upstream anti-turbulence screen. A layout of these thermocouples is found in **Figure 3**. These measurements provide an expedient inexpensive first-look at how well the NTF approaches the desired temperature uniformity requirements.

The settling chamber temperature measurements were made over the operating range of the NTF up to a dynamic pressure of 3500 psf. Data presented in **Figure 4** and **Figure 6** show the offset of the reference temperature measurement and the temperature variation, respectively, over a range of Mach and Reynolds numbers at three tunnel temperatures. Each symbol corresponds to an individual data point taken at one condition. The reference temperature offset was determined by subtracting the reference temperature measurement (made using a platinum resistance temperature device located in the settling chamber downstream of the cooling coils and the four anti-turbulence screens) from the average settling chamber temperature calculated from all the measurements on the thermocouple

Parameter	Low Speed Requirements	Transonic Requirements
<u>Total Temperature</u>		
Reference	1 deg F	1 deg F
Distribution	1 deg F	1 deg F
<u>Fluctuations</u>		
Turbulence	0.05%	0.05%
Noise	0.3% qinf	0.3% qinf
<u>Stream Angle</u>		
2-sigma along span	0.1 deg	0.1 deg
Gradient	0.014 deg/ft	0.023 deg/ft
<u>Mach Number</u>		
Reference	0.0004 (M=0.3)	0.0005 (M=0.8)
Gradient	4x10 <sup>-9</sup> /ft (M=0.3)	2x10 <sup>-9</sup> /ft (M=0.8)
<u>Stability</u>		
Total Pressure	3 psf (M=.3, P <sub>r</sub> = 5 atm)	5.5 psf (M=.8, P <sub>r</sub> = 5.5 atm)
Static Pressure	3 psf (M=.3, P <sub>r</sub> = 5 atm)	5.5 psf (M=.8, P <sub>r</sub> = 5.5 atm)
Total Temperature	1 deg. F	1 deg. F

**Table 3 – Flow Quality Requirements**

grid. The temperature variation was represented for the purposes of this paper as twice the standard deviation of the temperature measurements made with the thermocouple grid. In both figures, the dashed-line box highlights the requirements for the accuracy and variation.

**Figure 4** shows that the reference temperature accuracy appears to meet requirements at the warm temperature (120 F), but is outside the requirements at the cryogenic conditions (-150 F and -250 F). Furthermore, the reference temperature accuracy seems to get worse at the higher Mach numbers, up to a maximum bias error of 8 F. Closer examination of the temperature variation across the settling chamber reveals a possible source of this bias. **Figure 5** shows the constant temperature contours in the settling chamber for a typical high Mach number cryogenic condition. Although some of the temperature contours are highly subjective due to the thermocouple layout, it does appear that the coldest gas temperatures are concentrated at the bottom of the settling chamber, which coincides with the reference temperature measurement location.

The temperature variations shown in **Figure 6** reveal that the temperature variation in the settling chamber is greater than desired at all conditions, and that the variation increases with increasing Mach number. The data in **Figure 6** combines repeatability, bias, and gradients into a single number for comparison to the requirements. This technique of reducing these separate types of variation into one number can limit the understanding of the data.

#### Turbulence and Noise Characterization

Fluctuating pressure measurements in the NTF have been made using wall-mounted fast-response pressure transducers at several tunnel locations from the contraction region through the high-speed diffuser. **Figure 7** shows the ratio of rms values of the fluctuating pressure measurements (integrated from 1 Hz up to 150 Hz) to the test-section dynamic pressure as a function of tunnel location for four combinations of dynamic pressure and Mach number (two transonic and two supersonic conditions). For the two transonic Mach numbers, the pressure fluctuations are

on the order of 0.3% of the test-section dynamic pressure, and are consistent from the test-section through the high-speed diffuser. At the supersonic conditions, the pressure fluctuation level jumps up to 0.5% at the arc-sector fixed fairing (at the downstream end of the test-section) and in the high-speed diffuser, but decreases to about 0.1% in the test-section. This drop in test-section pressure fluctuation levels can be explained by the presence of a shock at the downstream end of the test-section at the supersonic conditions which prevents disturbances from propagating upstream. This pressure fluctuation data, obtained recently at the NTF, agrees with similar data taken previously in the NTF ( $\text{Igoe}^2$ ).

#### Flow Angle Characterization

Currently no information is available for the local flow angle distribution across the test-section in the NTF. However, information does exist on the integrated flow angle, calculated using upright and inverted runs of numerous models. Recently this information was plotted for similar models at similar test conditions to determine the stability of the flow angle over time. These data, shown in **Figure 8**, show clear signs of a change occurring in the tunnel flow angle brought about by the removal of a splitter plate attached to the arc-sector fixed fairing. This splitter plate, shown in **Figure 9b**, extends the chord of the arc-sector/fixed fairing (**Figure 9a**) and was added during a recent tunnel shutdown. When this large change in flow angle was noted, there was concern the calibration of the tunnel, done without the splitter plate installed, may have been affected. Therefore, the splitter plate was removed to return the tunnel to the configuration at which it had been calibrated. Subsequent tests showed that the integrated flow angle returned to its historical value of approximately 0.14 degrees for a transport model at transonic conditions. This instance proved the worth of charting tunnel data over time.

#### Mach Number Characterization

The tunnel has been recently calibrated for both the slotted- and solid-wall configurations. The slotted-wall calibration covered the test-envelope up to a dynamic pressure of 3500 psf, while the solid-wall calibration was limited

to a maximum Mach number of 0.45. Both calibrations were made using a 3-inch diameter centerline pipe that has four rows of static pressure orifices spaced 90 degrees apart. A sketch of this centerline pipe mounted in the tunnel, along with the pressure orifice layout, is shown in **Figure 10**. Data from the centerline pipe were used to calculate a Mach number correction (adjusting the reference Mach number to the centerline value) and to determine the Mach number longitudinal gradient (used in the calculation of buoyancy drag corrections).

**Figure 11** shows an example of the calibration data for a given test condition. At each calibration test condition, three back-to-back points were taken. The 95% confidence intervals are provided for each pressure orifice measurement, based on the variation in the three back-to-back measurements. It is evident from **Figure 11** that the variation between orifices is much greater than the variation between data points. Previous tests of this centerline pipe were made where the pipe was moved longitudinally in the test-section. It was noted that the pattern of variation between orifices moved with the centerline pipe location, indicating that this variation is caused by imperfections in the orifices. The initial calculation of Mach number variation, described below, deals only with the variation between points. Further work will be done later to incorporate the orifice bias error into the Mach number variation.

The Mach number variation was calculated by pooling the variance for all centerline pipe measurements made within the model test volume. The test volume for the slotted-wall configuration shown in **Figure 10** extends from test-section station 10 (test-section stations measured in feet from the start of the test-section) to station 16. The solid-wall test region extends from test-section station 9 to station 17. The Mach number variation for the slotted-wall test-section configuration is shown in **Figure 12**. Again, the dashed-line box highlights the accuracy requirements. As seen, based on short-term repeatability the Mach number accuracy requirements are being met for almost all conditions (the exception being at some supersonic conditions).

The NWTC requirements on the longitudinal Mach number gradients are based on the desire for a buoyancy drag correction of one drag count or less. Therefore, the buoyancy drag correction for each calibration test condition was calculated for a typical NTF model, having a model volume of 0.884 ft<sup>3</sup> and a reference area of 2.6 ft<sup>2</sup>. The results for the slotted-wall calibration are shown in **Figure 13**. This plot indicates that requirements for buoyancy drag are being met in the transonic region (for which the tunnel was designed), and are not met at the low-speed and supersonic conditions. Again, further work will be done to assess the effect of the orifice bias errors on these calculations.

#### Tunnel Stability Characterization

**Figures 14** and **Figure 15** plot the stability over time of total and static reference pressure measurements and the reference temperature measurement for a low-speed and transonic cryogenic condition. To measure the stability, the tunnel was held on a condition while data points were taken over a period of time. The time-span was 1.5 minutes for the low-speed condition and 2 minutes for the transonic case. During this period, nine data points were obtained, and are those shown on the plot. The total pressure stability was within the required limits for both the low-speed and transonic conditions. The static pressure stability met the requirements at the low-speed condition, but exceeded the limits at the transonic condition. Conversely, the temperature stability was within limits transonically, but slightly out of tolerance for the low-speed case. To adequately characterize the temperature stability for the low-speed condition, though, a larger timeframe of data is required, as the temperature limits of the temperature fluctuation do not appear to have been reached.

#### Data Quality Assurance Program

Historically, facility personnel were trained to detect and correct blunder-type errors and abnormally large data scatter. In addition, single-point calibration methods were used for making major corrections. Assessment of repeatability was based on relatively short-term, small sample, methods which are incapable of determining measurement

stability and yield so few degrees of freedom that they cannot reliably assess measurement uncertainty nor point to potential improvements unless the effects are much larger than the normal scatter. The initial effort in the new data quality assurance (DQA) program, which was completed in FY99, was to find an appropriate measurement assurance methodology, to train the staff in its use, and to begin implementation. The only credible approach with the necessary traceability seems to be the Measurement Assurance concept developed for calibration laboratories by NIST and extended for wind-tunnel testing by Langley Research Center. The key elements of this concept are

- (a) Statistical quality control for measurement (Shewhart<sup>3</sup>),
- (b) Application of Shewhart's statistical methods to both short- and long-term repeatability (Eisenhart<sup>4</sup>),
- (c) Periodic testing of stable artifacts (check standards) and the use of Shewhart's control charts on the results to determine the measurement system stability (Pontius and Cameron<sup>5</sup>),
- (d) Repeat-data sets during a customer test, together with appropriate scaling, for comparison with the check standard results (Schumacher<sup>6</sup>),
- (e) A standard method for referencing to a common state (free-air). The standard used at the NTF is the wall-signature method.

Currently, the NTF is running check standards periodically and assessing the short- and long-term repeatability for attached flow over the model on statistical control charts. Repeat-run sets are also obtained at the beginning and end of each customer test for comparison with the suitably-scaled check standard results. In addition, pre-test predictions and post-test statements of repeatability are provided to the customer.

Check standard model testing.

The check standard model for the NTF (shown in **Figure 16**) is a subsonic transport model that is no longer used for any other kind of testing. The balance used is the LaRC NTF 113C that is a one-piece moment-type. The model geometrical characteristics and balance full-scale limits are given in **Table 4**.

S, ft <sup>2</sup>	1.988
$\bar{c}$ , in.	5.74
b, in.	52.97
N, lb <sub>t</sub>	6500
A, lb <sub>t</sub>	400
PM, in.-lb <sub>t</sub>	13,000

**Table 4 – Model and Balance Specifications**

A minimum of four repeat-run sets is obtained by the facility each year. A repeat-run set is called a “group” and consists of the following runs back-to-back at the same test conditions:

- Inverted polar
- Upright pitch polar
- Upright pitch polar
- Upright pitch polar
- Inverted polar

The first two runs and the last two runs form a two-observation group that is used to estimate the short-term repeatability of the flow angularity. The middle three runs are used to form a three-observation group that is used to estimate the short-term repeatability of the pitch-plane uncorrected balance coefficients  $C_{N_u}$ ,  $C_{A_u}$ ,  $C_{m_u}$ . Long-term repeatability (and stability) is estimated from the variation of the group averages over time. The short- and long-term repeatability groups are analyzed for measurement stability and scatter level (precision) using so-called Three-Way statistical control charts.

Too few repeat-sets have been taken so far to definitively state the behavior of instrument scatter (precision) as a function of test section conditions so the estimated short- and long-term standard deviations ( $\hat{\sigma}_{wg}$ ,  $\hat{\sigma}_{bg}$ ) presented in **Table 5** are pooled over the Mach and q range. The pooled degrees of freedom for  $\hat{\sigma}_{wg}$  (short-term) and  $\hat{\sigma}_{bg}$  (long-term) are approximately 40 and 20 respectively. The expected standard deviation for a single data point for attached flow (for the check standard) is the root-sum-square of  $\hat{\sigma}_{wg}$  and  $\hat{\sigma}_{bg}$ :

$$\hat{\sigma}_{one\ point} = \sqrt{\hat{\sigma}_{wg}^2 + \hat{\sigma}_{bg}^2}$$



Check standard probe testing

The repeatability assurance program described in the previous section for balance coefficients is applied in a similar manner to the repeatability of flow parameters, specifically Mach number and dynamic pressure,  $q$ . The method used is to obtain repeat data for a probe (shown installed in **Figure 17**) in an empty test section (low-speed and transonic tunnels) or a wall pressure upstream of the model area (supersonic tunnels). A group consists of three back-to-back repeat measurements at a single test condition. The following ratios are computed:

$$C_q = \frac{q_{centerline}}{q_{reference}}$$

$$C_M = \frac{M_{centerline}}{M_{reference}}$$

where the centerline and reference values are computed using the total and static pressures from the probe and the reference system respectively. The repeatability of  $C_q$  and  $C_M$  expresses the variation associated with the test section itself and both sets of static and total pressure propagated into the formulas for computing Mach and  $q$ .

Two check standard tests with a total of 63 groups over 12 test conditions have been

conducted in the NTF. In the future, it is expected that four such tests will be conducted each year. Although two tests is considered insufficient to declare the measurement system + test section to be in statistical control, we will use the pooled values obtained so far to estimate the repeatability for Mach and dynamic pressure as shown in the **Table 6**. The pooled degrees of freedom for the within-group and between-group standard deviations,  $\hat{\sigma}_{wg}$  and  $\hat{\sigma}_{bg}$ , are 126 and 51 respectively. The standard deviation for a single data point is the root-sum-square of  $\hat{\sigma}_{wg}$  and  $\hat{\sigma}_{bg}$ :

$$\hat{\sigma}_{one\ point} = \sqrt{\hat{\sigma}_{wg}^2 + \hat{\sigma}_{bg}^2}$$

The estimated uncertainties of the tunnel calibration data are believed to be about the same as the values given in **Table 6**. Check standard data have been obtained so far for  $930\ psf \leq q \leq 3000\ psf$ . For conditions outside of this range, the scatter may be somewhat higher.

Support of the Implementation of Wall Interference Corrections

The NTF characterization effort also provides information to support the development and implementation of wall interference correction codes for the NTF. This support includes wall pressure data, wall boundary layer

Uncorrected coefficient	$\hat{\sigma}_{wg}$	$\hat{\sigma}_{bg}$	$\hat{\sigma}_{one\ point}$
$C_{A_u}$	0.00002	0.00015	0.00015
$C_{N_u}$	0.00052	0.0022	0.0022
$C_{m_u}$	0.00030	0.00056	0.00064

**Table 5 – Check Standard Model Short- and Long-term Variation**

	Within-group	Between-group	One-point
$\hat{\sigma}_q / q$	0.00036	0.0017	0.0017
$\hat{\sigma}_M / M$	0.00022	0.00092	0.00095

**Table 6 – Check Standard Probe Short- and Long-term Variation**

information, and check standard model data. The following sections provide the status of this support effort, as well as presenting a summary of the status of the wall interference correction effort.

#### Wall Pressures

In the last couple of years, the wall pressure measurement system at the NTF has been improved to provide the high-quality wall pressure signatures necessary for the implementation of wall interference correction codes. Empty tunnel wall pressure signatures have been obtained for both the solid- and slotted-wall test-section configurations.

#### Wall Boundary Layer Height

Wall boundary layer measurements have been made in the NTF for both the solid- and slotted-wall test-section configurations. **Figure 18** shows a sketch of the boundary layer rake design used for these measurements. For the slotted-wall configuration, two tests were run to provide boundary layer information at the seven different test-section locations shown in **Figure 19**. These locations were chosen to provide data on both the longitudinal boundary layer growth in the test-section, and the boundary layer uniformity at a given test-section station. Currently boundary layer data for the solid-wall test-section configuration is only available for the farside wall at station 12.77. A sample of the data is shown in **Figure 20** and **Figure 21**. In both of these figures, the data presented as the average of a combination of the measurements made over a small region of the NTF low-speed envelope, with error-bars denoting the variation at each location. The purpose for presenting the data in this fashion is to provide a general magnitude of the boundary layer height, longitudinal growth rate, and uniformity. **Figure 20** reveals that the boundary layer height averages between 3 and 4 inches at test-section station 13 over this range of conditions. At these same conditions, it is seen in **Figure 21** that the boundary layer grows from about 1.2 inches in the contraction region up to 3-4 inches at station 13 (the center-of-rotation for both sting-mounted and sidewall-mounted models).

This boundary layer height information has been used in the development of semi-span model stand-off geometry and for calibration of

a computational fluid dynamics (CFD) model of the NTF test-section.

#### Implementation of WICS in the NTF

The Wall Interference Correction System (WICS) code (Ulbrich<sup>7</sup>) originally developed for the Ames 12-Foot Pressure Wind Tunnel has been implemented in the NTF for use during solid wall testing. WICS-generated wall-interference corrections to an equivalent free-air flow field are computed using the wall-pressure signature method combined with balance measurements of model forces and moments. Mean corrections for tunnel blockage and upwash are determined and are then applied to the tunnel parameters. The code also provides the wall interference *variation* in the vicinity of model in the form of contour plots; this aerodynamic analysis-enhancing capability is generally unavailable from simpler classical methods. The code has been used in an off-line mode for semispan tests, and will be operational for fullspan testing in the first quarter of 2000. Because the method is fast and robust, it is well-suited for real-time or near real-time application. Efforts are currently underway to implement WICS for online post-point corrections.

Sample interference predictions from a recent large-model NTF test are presented in **Figure 22** and **Figure 23**. Here, uncorrected, the classically corrected (AG-336, 1998), and the WICS-corrected solid wall measurements are compared with slotted-wall measurement obtained on the same model. Since the NTF was designed to minimize wall interference effects, the uncorrected slotted wall results, though not absolutely free of wall effects, should provide a good baseline from which to reference the correction. Effects included in the classical corrections are those due to blockage (solid and attached wake), lift, and streamline curvature, while WICS includes these and additional effects due to any separation of the model wake. **Figure 22** presents the lift correction, indicating an expected, large, lift-curve slope increase for the uncorrected solid wall data. Applying the corrections rotates the curve into alignment with the slotted-wall results. At low lift the two correction methods are in close agreement, however, at the higher angles of attack the difference between the methods widens to about 0.005 in  $C_L$ . Drag corrections are

presented in **Figure 23**. In the minimum drag region, as demonstrated by Ulbrich<sup>7</sup>, the WICS predictions are lower than those predicted by the classical methods by about 3-4 drag counts. At the higher drag values, the difference between the two methods widens to about 20 drag counts, indicating the presence of a separated wake. The planned addition of Maskell corrections (AG-336<sup>8</sup>) to the classical corrections is expected to narrow this difference significantly.

### Conclusions

A process has been developed and implemented for the characterization of the NTF that will provide verifiable flow quality and data quality that met customer expectations. This process provides information on the areas in which the NTF meets the target requirements, the areas that fall short of these requirements, and the areas where more information is needed before a credible conclusion can be made.

Currently, the NTF appears well within requirements on Mach number accuracy and longitudinal gradient based on short-term repeatability. However, work must be done to understand the effect of the scatter due to pressure orifice imperfections on these measurements. The tunnel stability (a measure of the controllability) again appears close to meeting requirements. Additionally, wall pressure signatures and boundary layer measurements are sufficient to aid the implementation wall interference corrections and computational modeling of the tunnel.

The main opportunity for possible improvement is in the NTF temperature measurement and control. First, though, test-section temperature distributions need to be obtained to determine whether the temperature variation levels in the settling chamber upstream of the anti-turbulence screens exist in the test-section. If they do, previous experience in cryogenic wind-tunnels has shown that the pattern of liquid nitrogen injection into the flow has a large impact on the temperature distribution and variation. In addition, the method for determining the reference temperature may be reviewed.

There are still several areas of the NTF characterization effort where more data is required. Information is especially lacking in regard to off-centerline test-section measurements. In addition, more data is needed for the check standard tests before an assessment can be made. Future characterization tests will be directed to meet these needs.

### Acknowledgements

I would like to acknowledge both Dr. Michael Hemsch of NASA Langley Research Center and William Krieger of Lockheed Martin, for their assistance with the preparation of the Data Quality Assurance section of this paper.

### References

1. Binion and Steinle, *Flow Quality Requirements Rationale and Measurement Technique*, CR95-017, March 1995.
2. Igoe, William, Analysis of Fluctuating Static Pressure Measurements in the National Transonic Facility, NASA TP-3475, March 1996.
3. Shewhart, Walter A., *Statistical Method from the Viewpoint of Quality Control*, Dover 1986. (originally published in 1939)
4. Eisenhart, Churchill, "Realistic Evaluation of the Precision and Accuracy of Instrument Calibration Systems", in *Precision Measurement and Calibration: Statistical Concepts and Procedures*, NBS SP-300, Vol. 1, Harry H. Ku, ed., February 1969, pp. 21-47.
5. Pontius, P. E., and Cameron, J. M., "Realistic Uncertainties and the Mass Measurement Process", in *Precision Measurement and Calibration: Statistical Concepts and Procedures*, NBS SP-300, Vol. 1, Harry H. Ku, ed., February 1969, pp. 1-20.
6. Schumacher, Rolf B. F., *Measurement Uncertainty - Measurement Assurance Handbook*, 1996 (published by the author)

7. Ulbrich, Norman, *The Real-Time Wall Interference Correction System of the NASA Ames 12-Foot Pressure Wind Tunnel*, NASA CR-1998-208537, July 1998.
8. Ewald, B.F.R. (Editor), *Wind Tunnel Wall Corrections*, AGARDograph 336, October 1998.

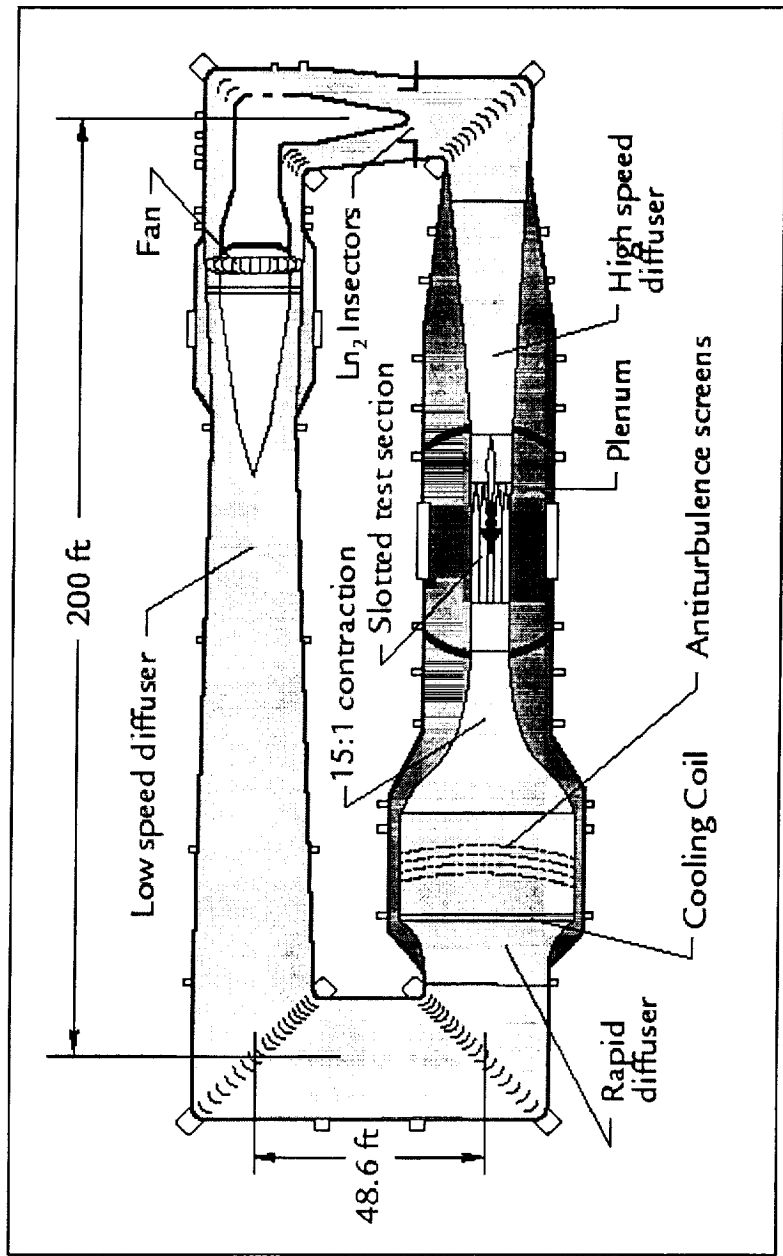


Figure 1 – NTF Circuit

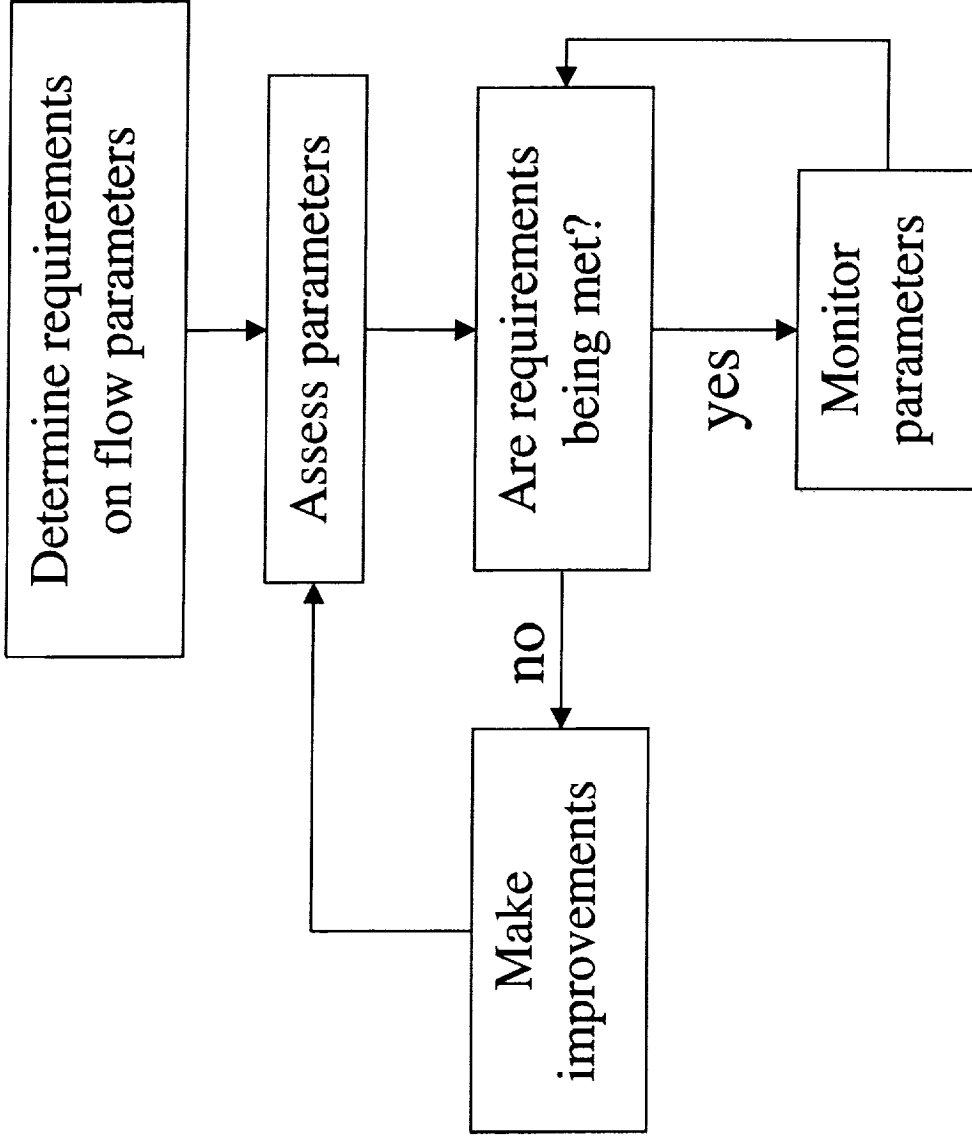


Figure 2 – Characterization Process

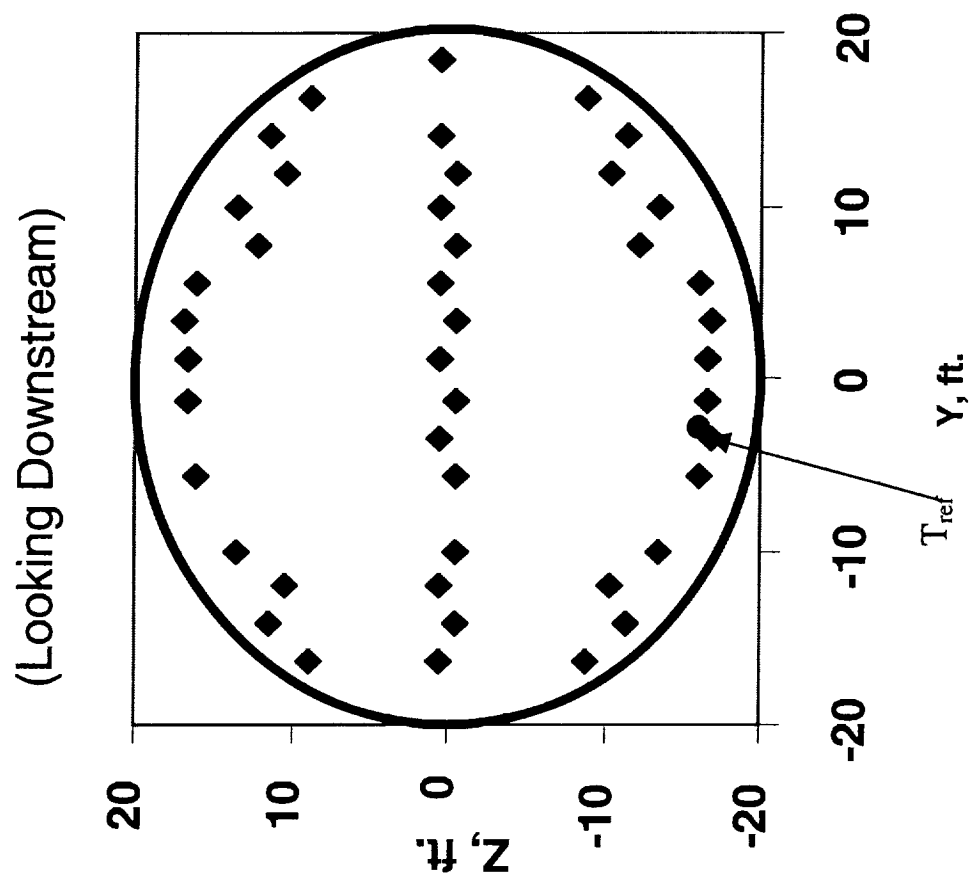


Figure 3 – Settling Chamber Thermocouple Layout

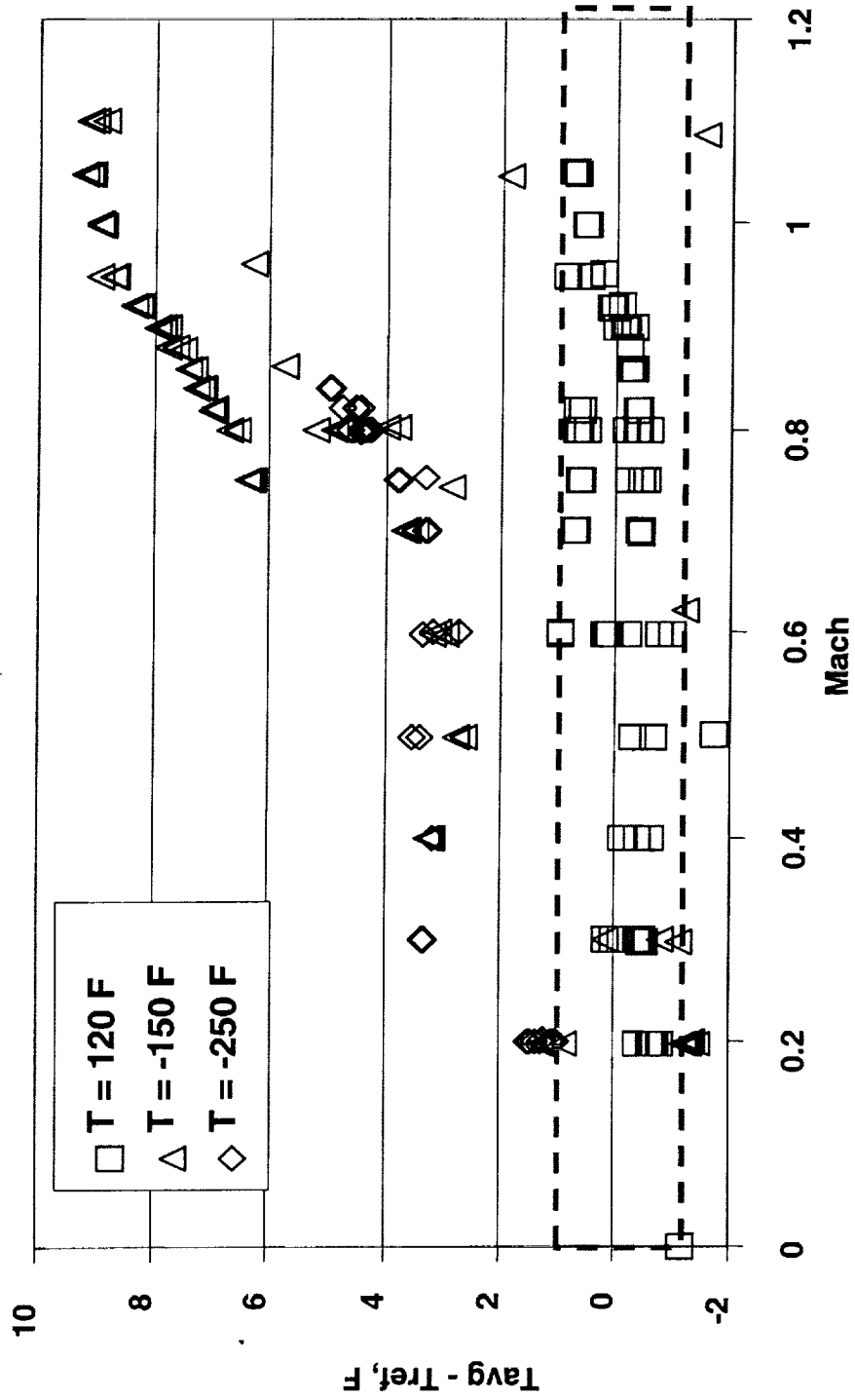


Figure 4 – Settling Chamber Temperature Offset



$M = 0.80$ ;  $T = -250$  F;  $P_T = 33.3$  psi

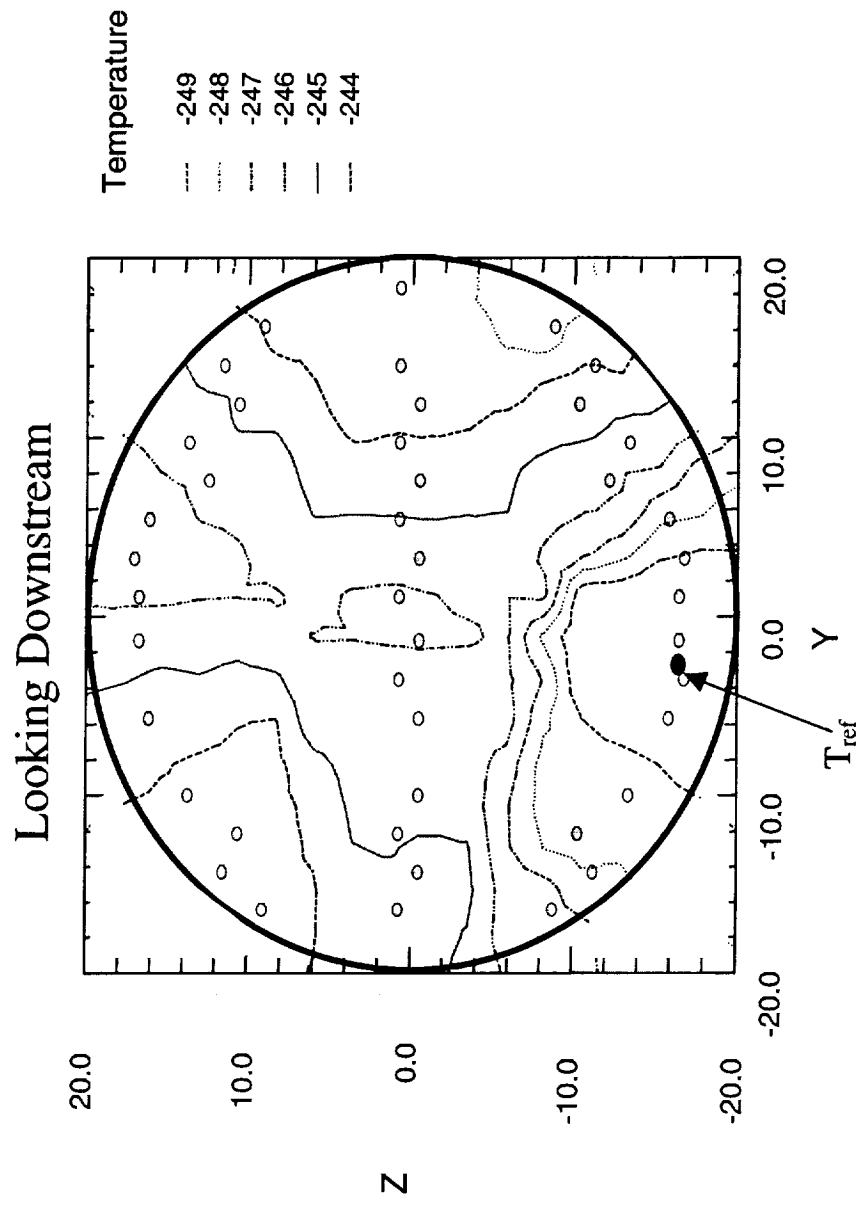


Figure 5 – Settling Chamber Temperature Contours

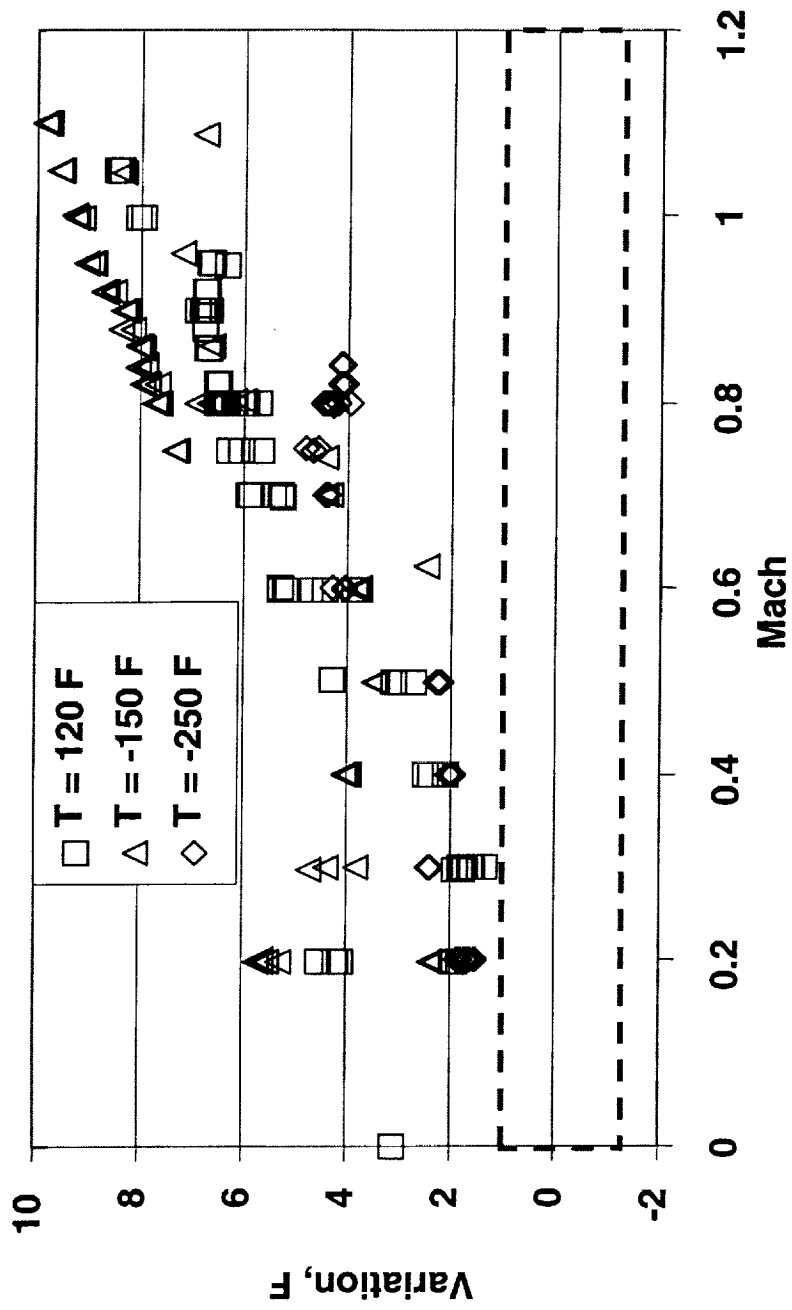


Figure 6 -- Settling Chamber Temperature Variation

Spectrum of RMS pressure ( P ) from KULITE integrated over frequency range 1-150Hz

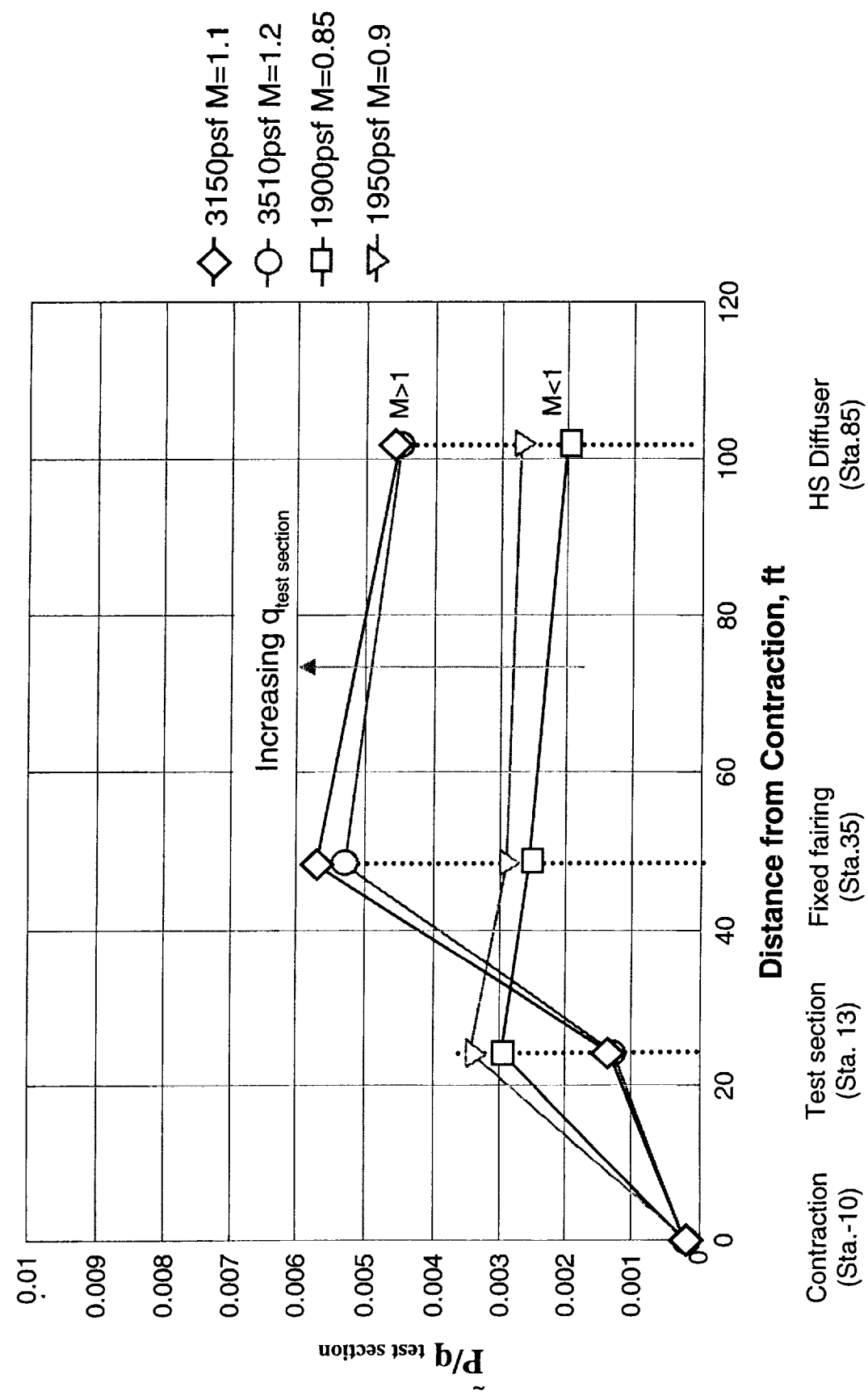


Figure 7 – NTF Pressure Fluctuation Levels

M = .80 to 0.855; q = 840 to 1900 psf; T = 120 F  
(Data from three different transport models)

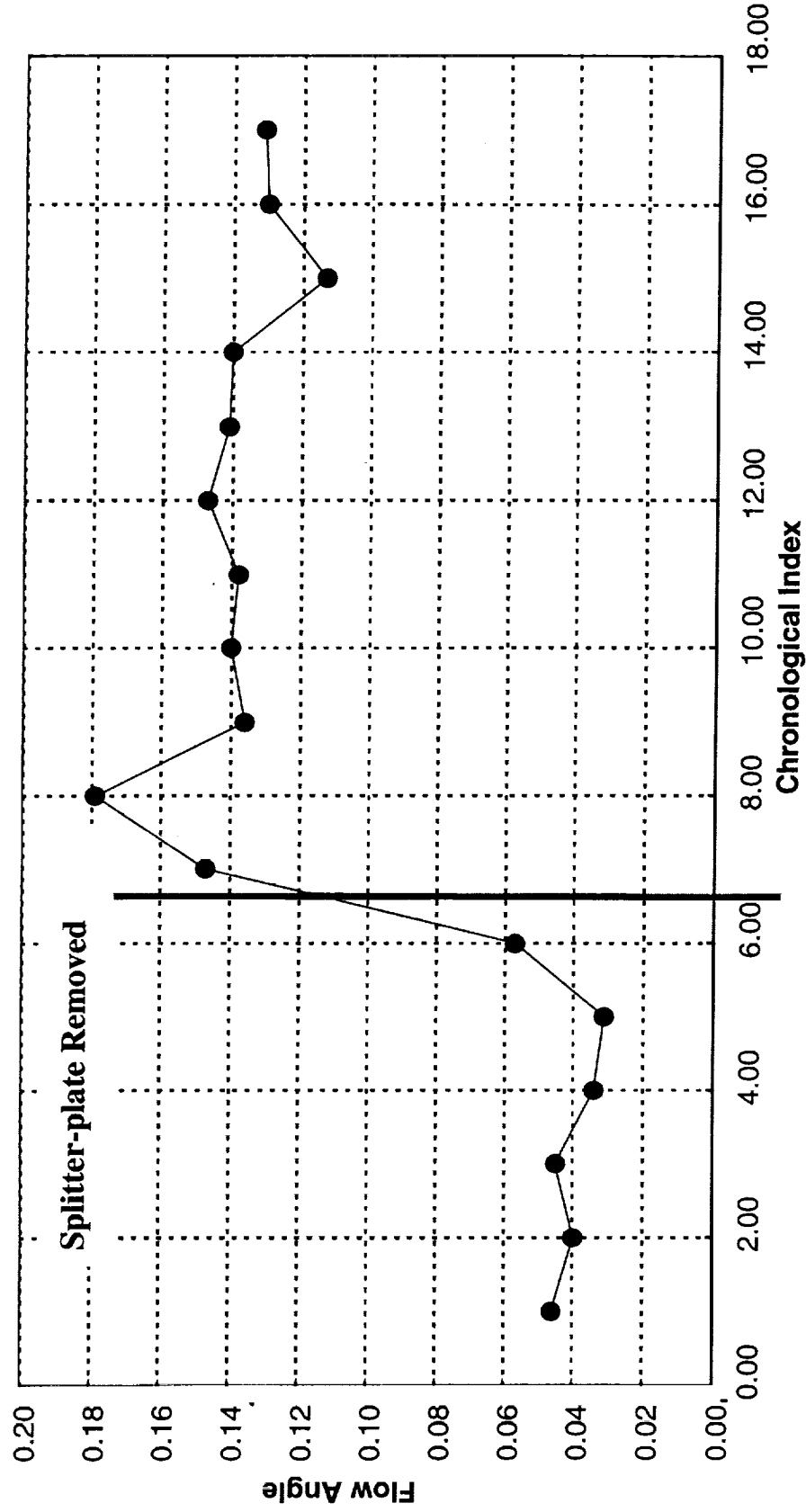


Figure 8 - Integrated Flow Angle

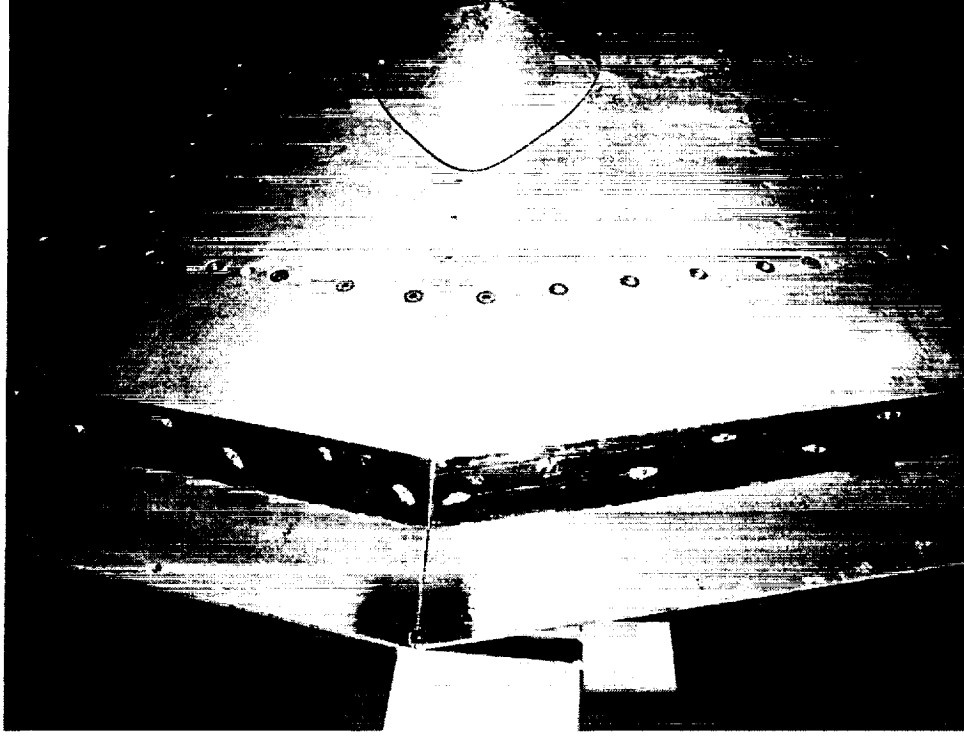
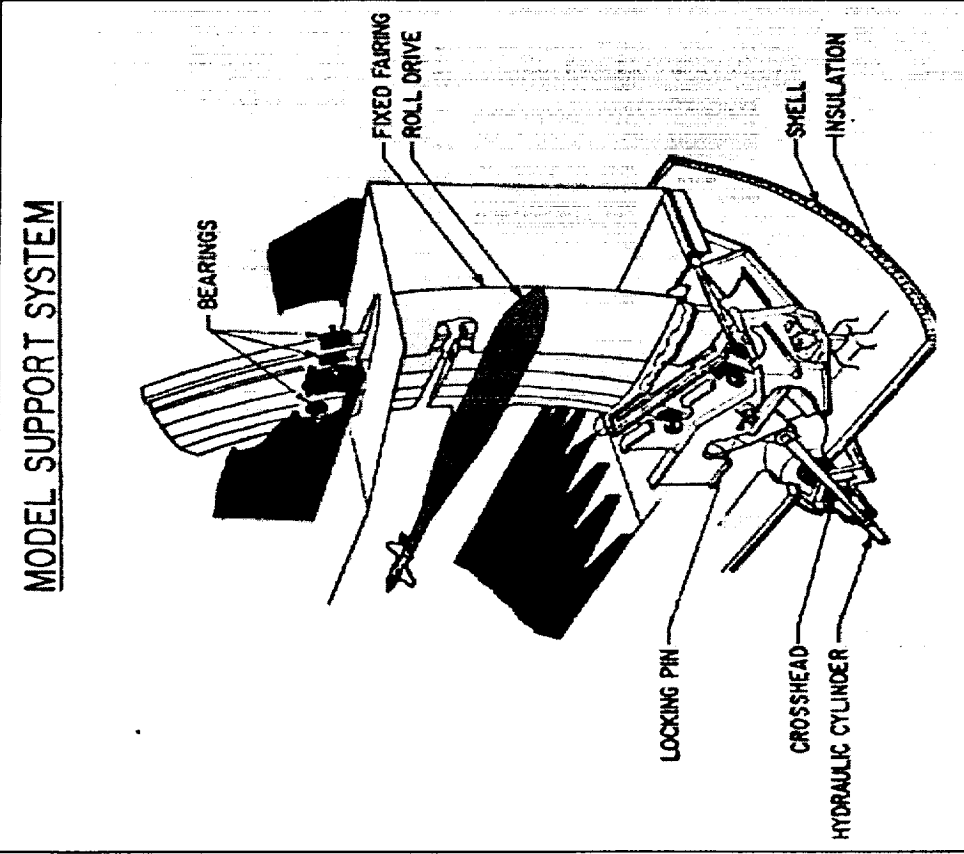


Figure 9a – NTF Model Support System

Figure 9b – Splitter-plate installed on fixed fairing

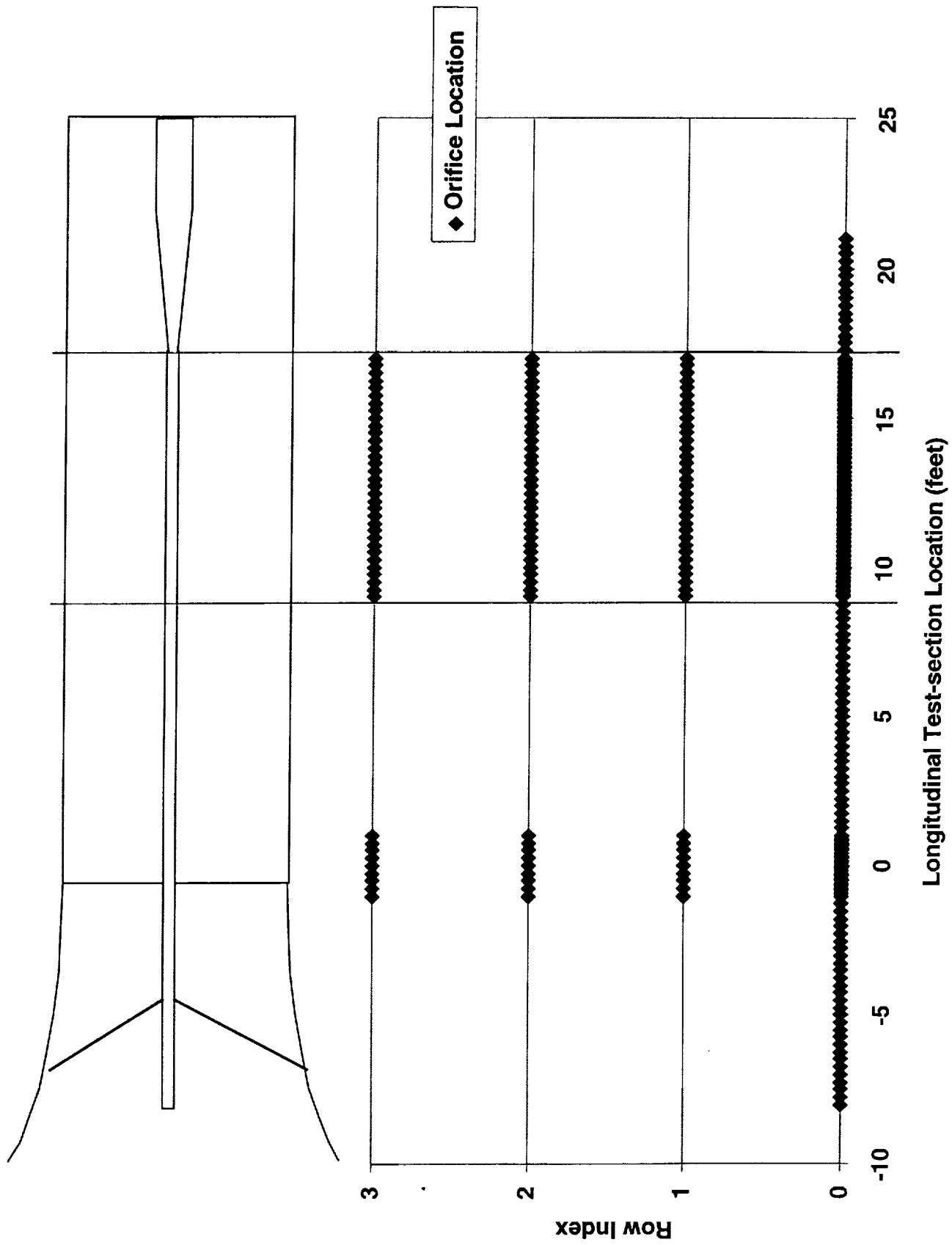


Figure 10 -- Centerline Pipe Installation

**M = 0.60; Re/ft =  $4.3 \times 10^6$ ; T = 120 F**

**Avg. of 3 points, with 95% Confidence Intervals**

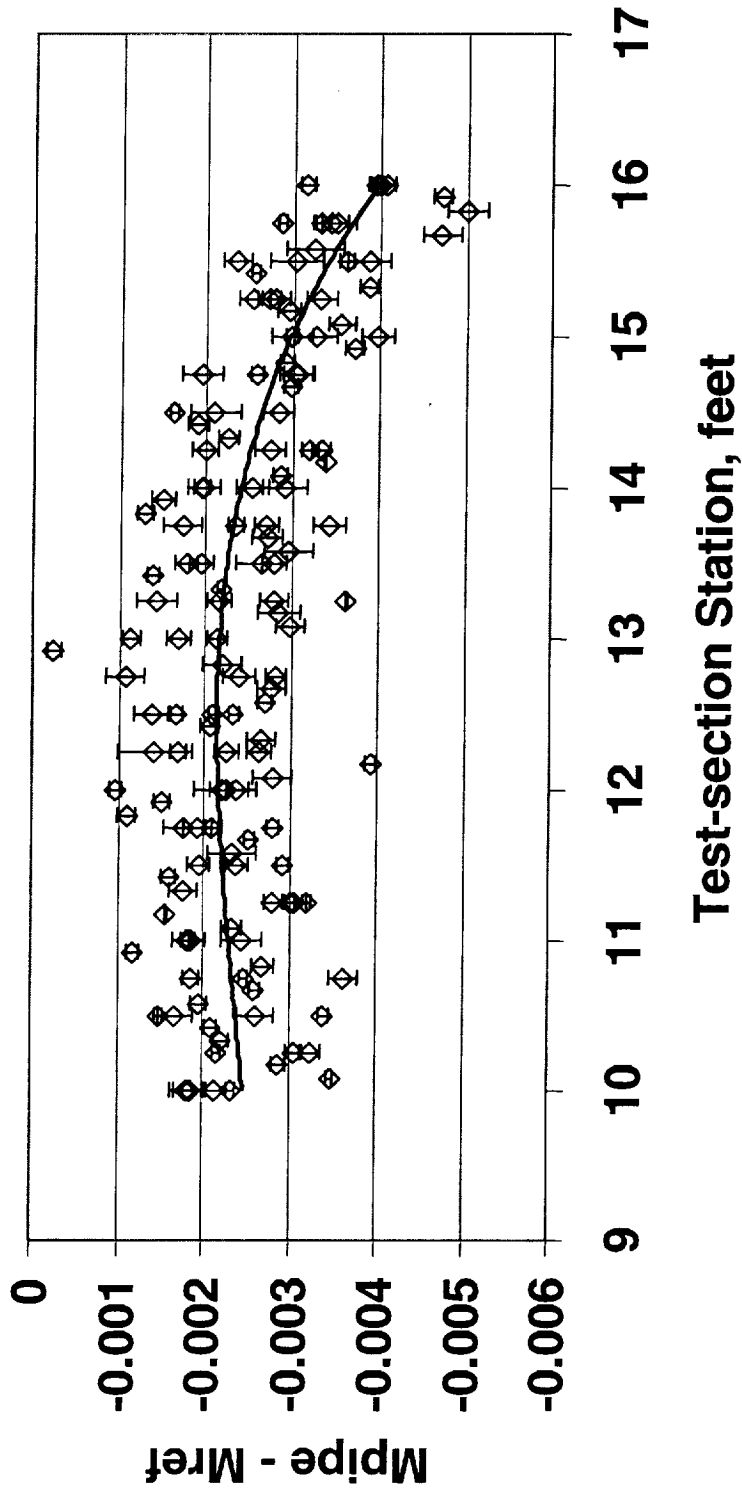


Figure 11 – Centerline Pipe Data from NTF Slotted-wall Calibration

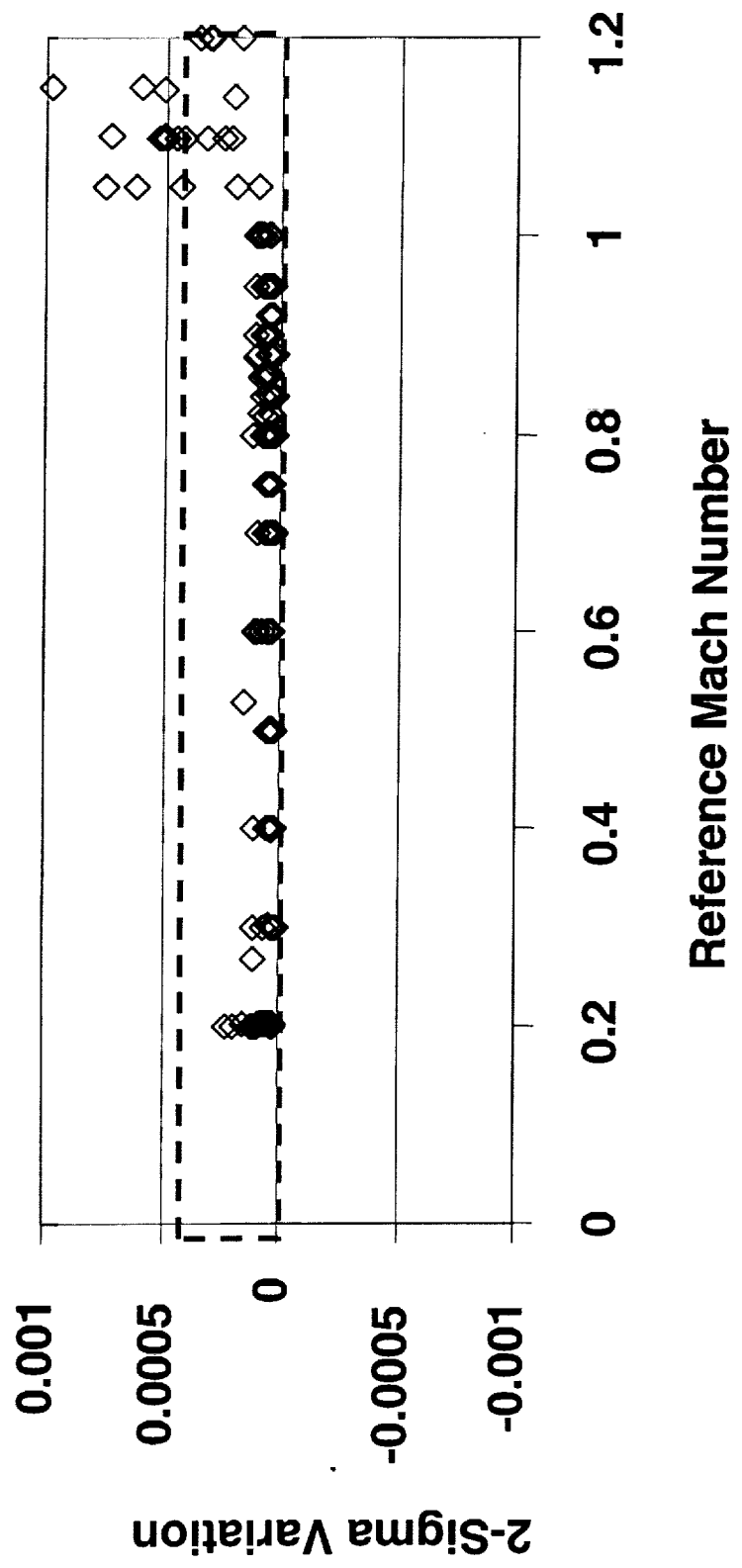
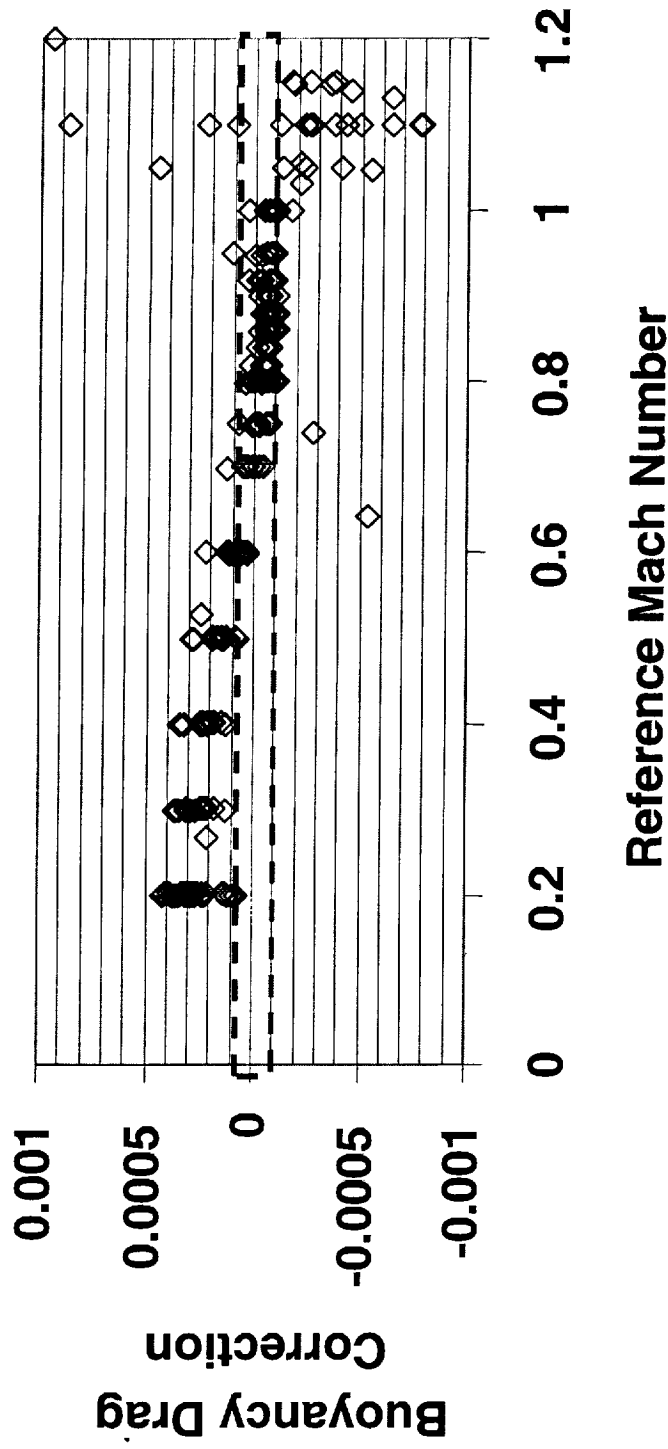


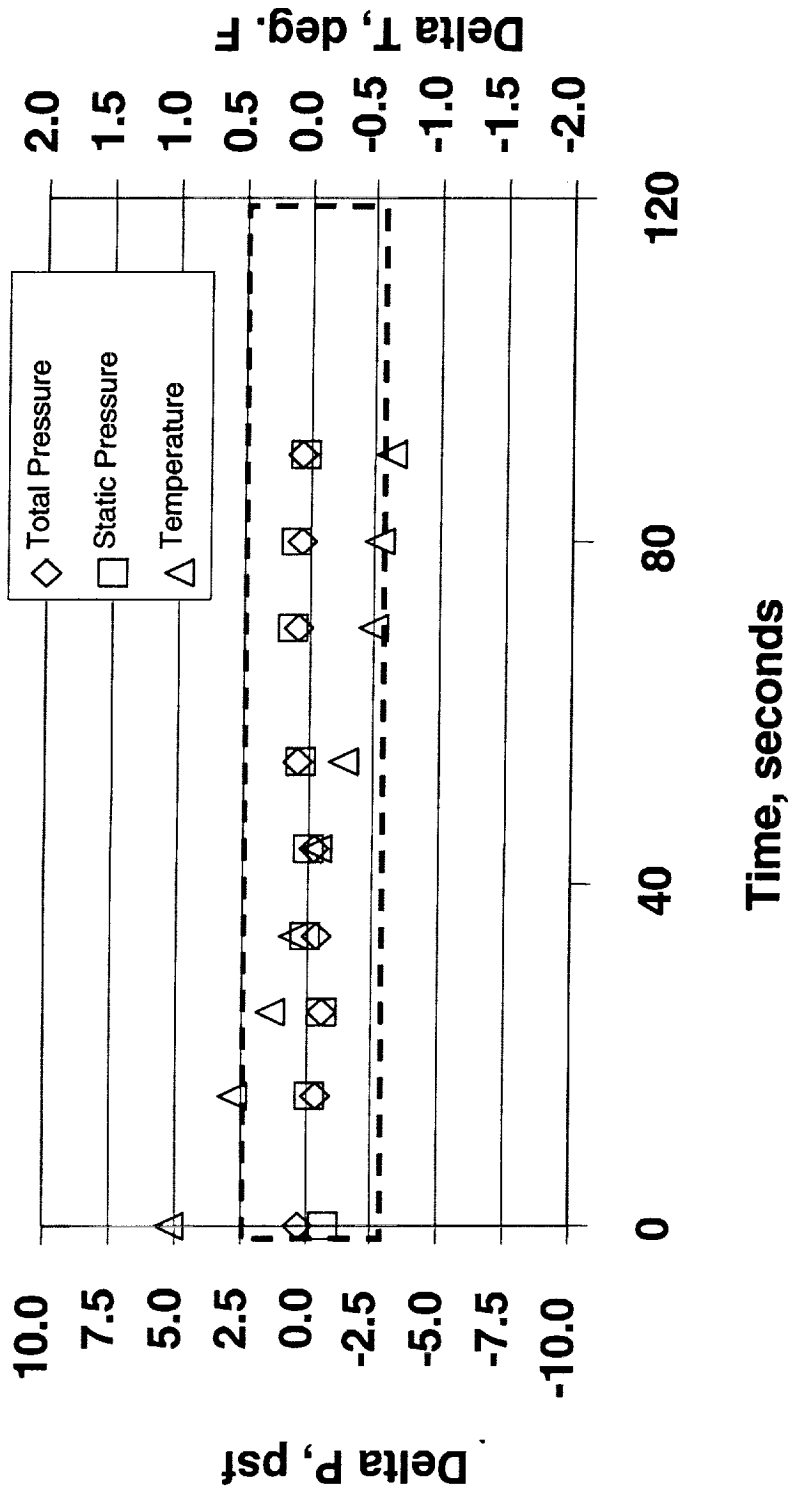
Figure 12 -- Slotted-wall Calibration Repeatability





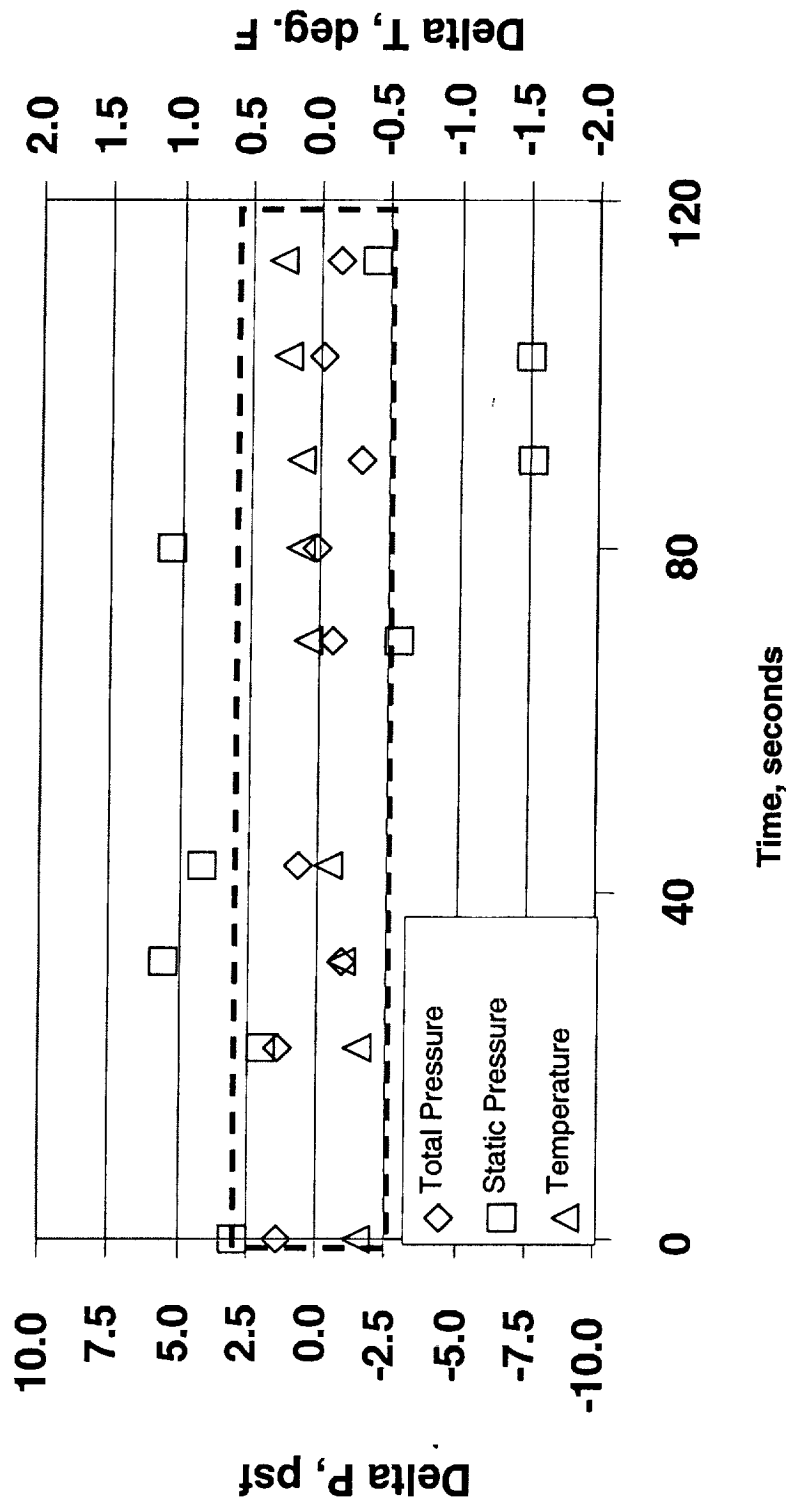
Calculations are for typical NTF full-span model;  $V = 0.884 \text{ ft}^3$ ,  $S = 2.6 \text{ ft}^2$

Figure 13 – Slotted-wall Calibration Buoyancy Corrections



$M = 0.30; T_T = -250 \text{ F}; P_T = 4 \text{ atm.}$

Figure 14 -- Tunnel Pressure and Temperature Stability, Low-speed



$M = 0.80; T_T = -250 \text{ F}; P_T = 4 \text{ atm.}$

Figure 15 - Tunnel Pressure and Temperature Stability, Transonic

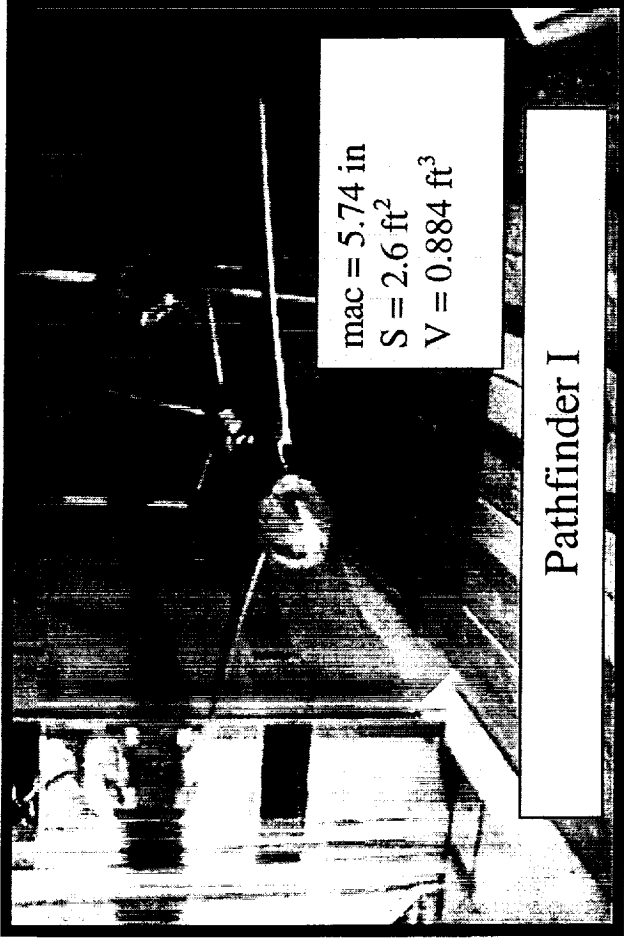


Figure 16 – NTF Check Standard Model

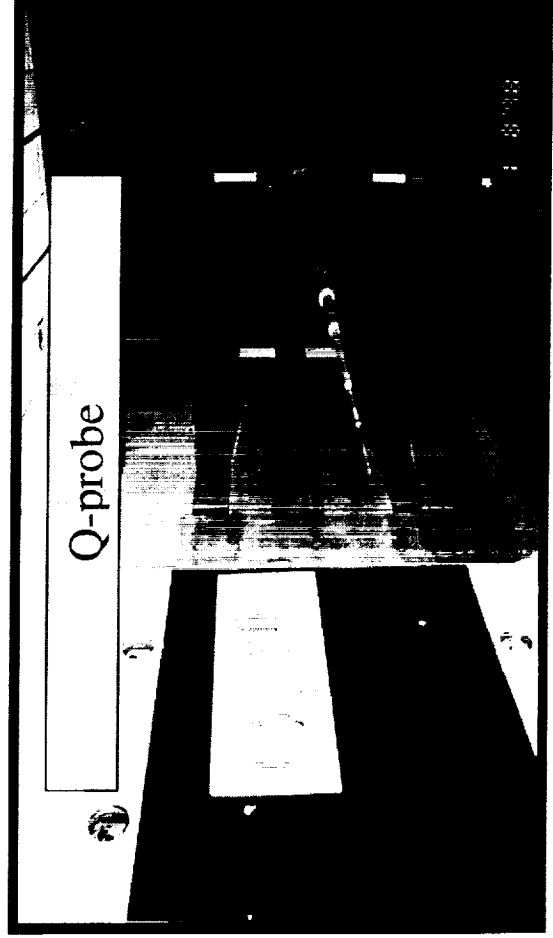
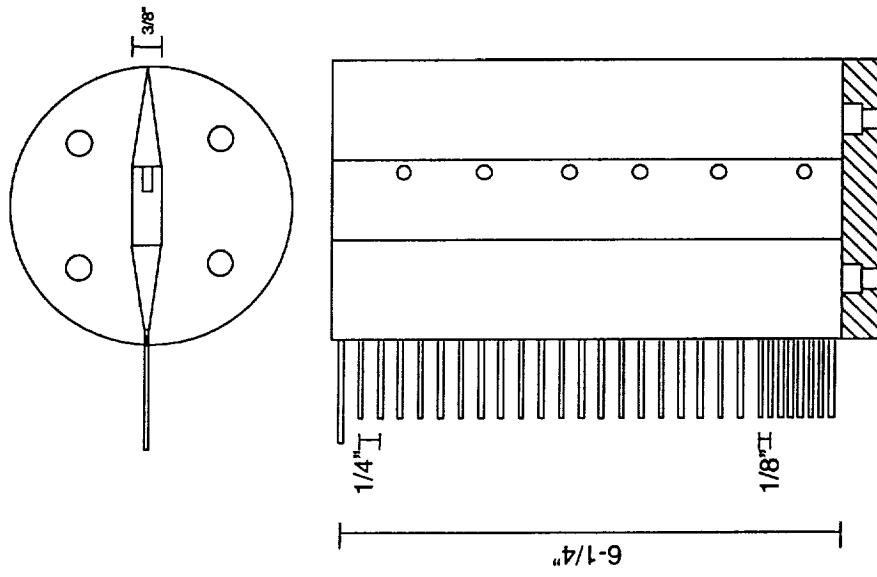
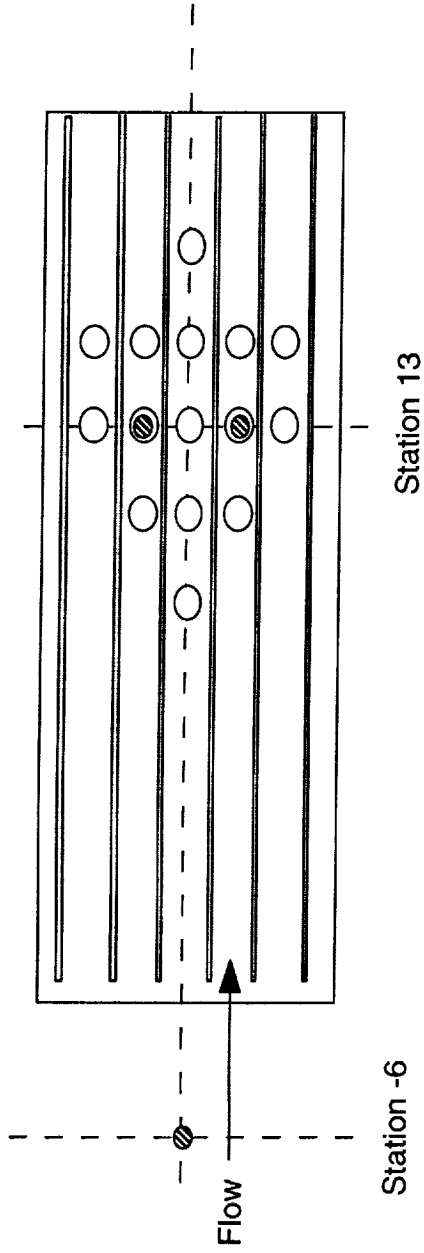


Figure 17 – NTF Check Standard Probe

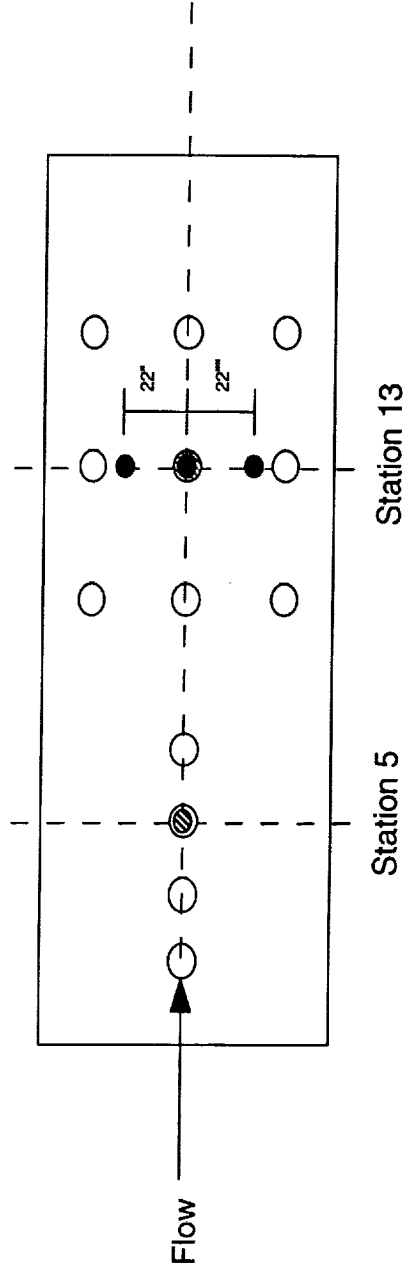


**Figure 18 – Boundary Layer Rake Design**

Test Section Ceiling



Test Section Far Side Wall



- Boundary Layer rake locations for test 104
- ▨ Boundary Layer rake locations for test 108B

Figure 19 – Boundary Layer Rake Locations

**M = .20 to .40**  
**Re/ft. = 2 to 8 Million**  
**T = 90 to 120 F**

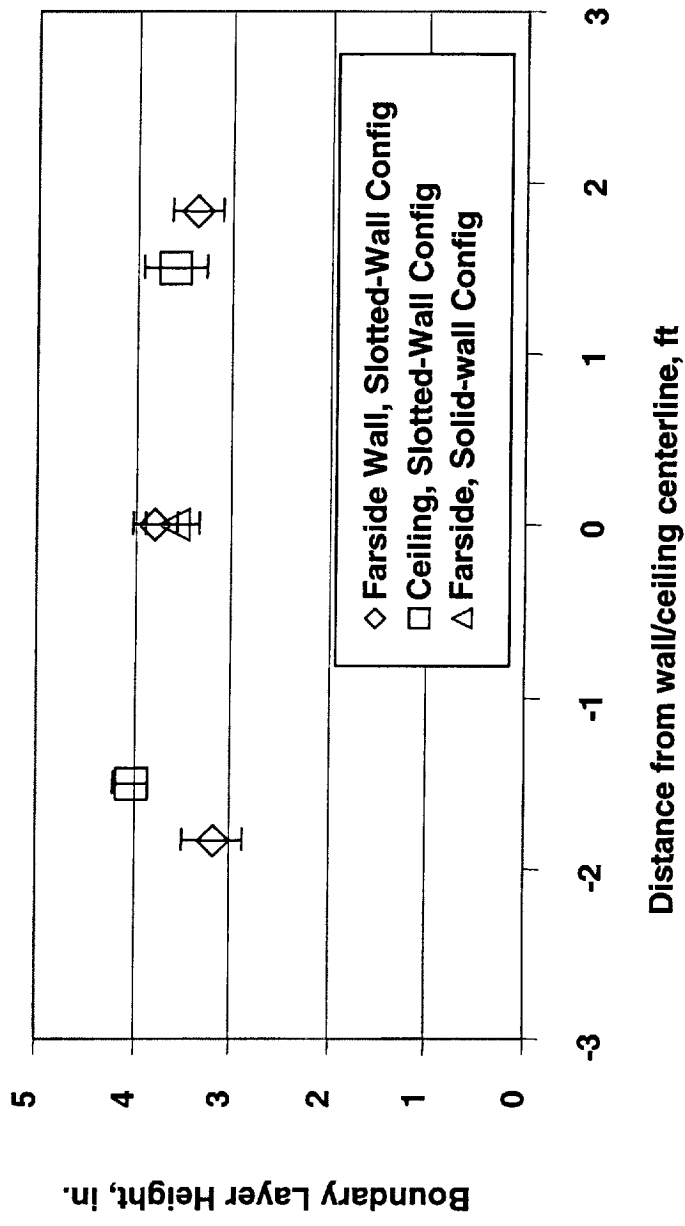


Figure 20 – Boundary Layer Uniformity, Station 13

M = .20 to .40  
Re/ft. = 2 to 8 Million  
T = 90 to 120 F

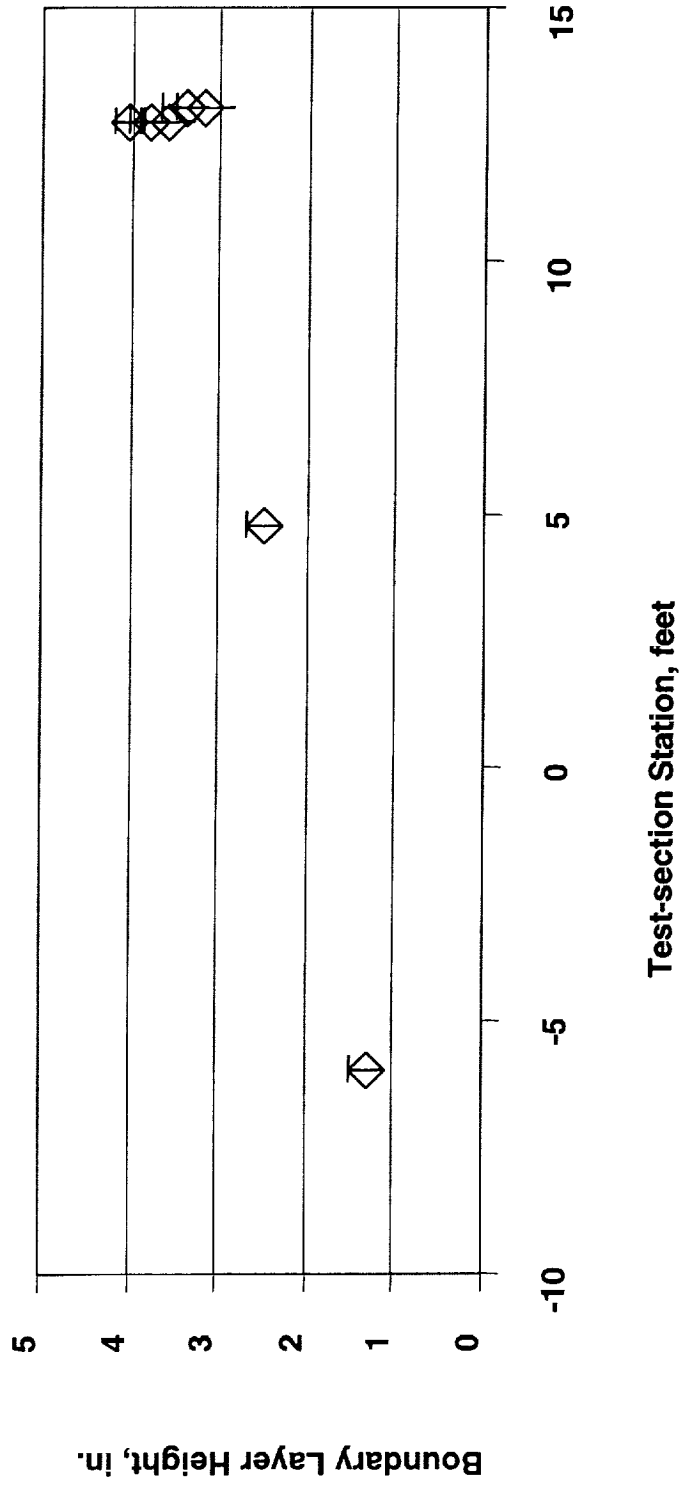


Figure 21 - Boundary Layer Longitudinal Growth



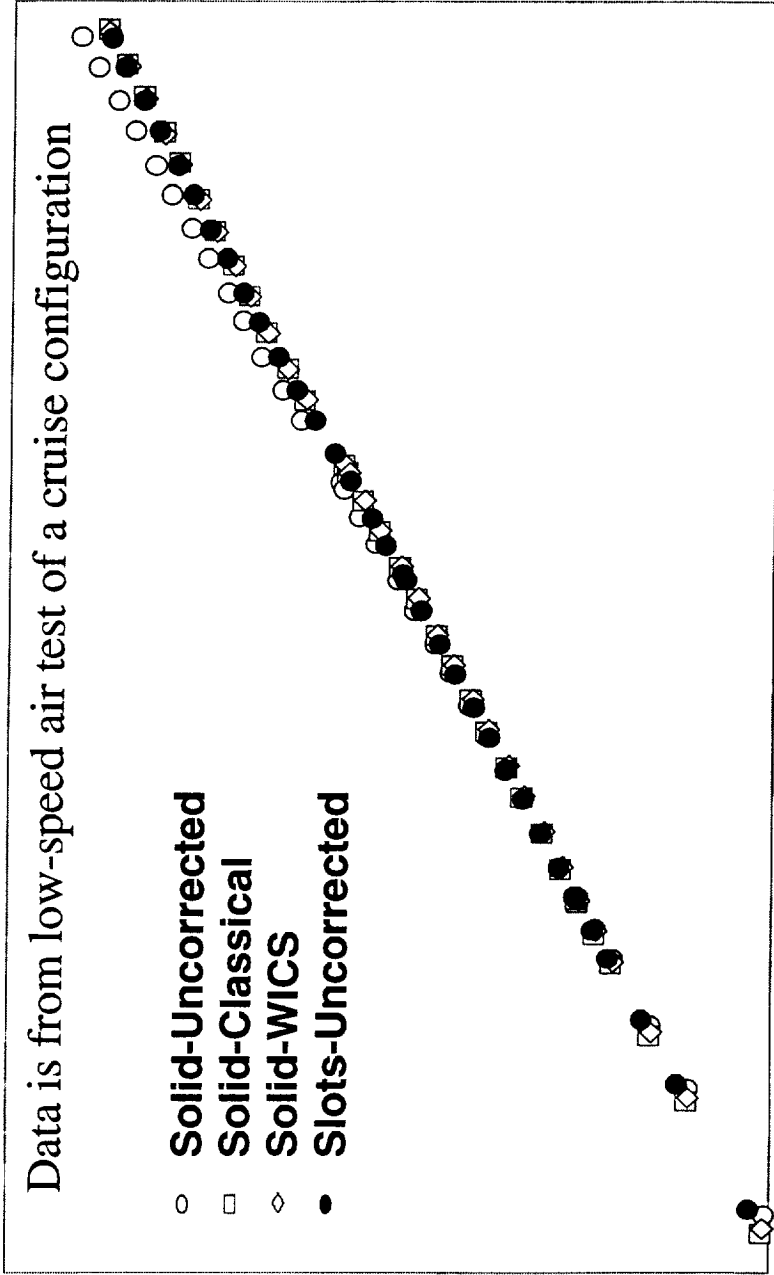


Figure 22 – Wall Interference Corrections, Lift

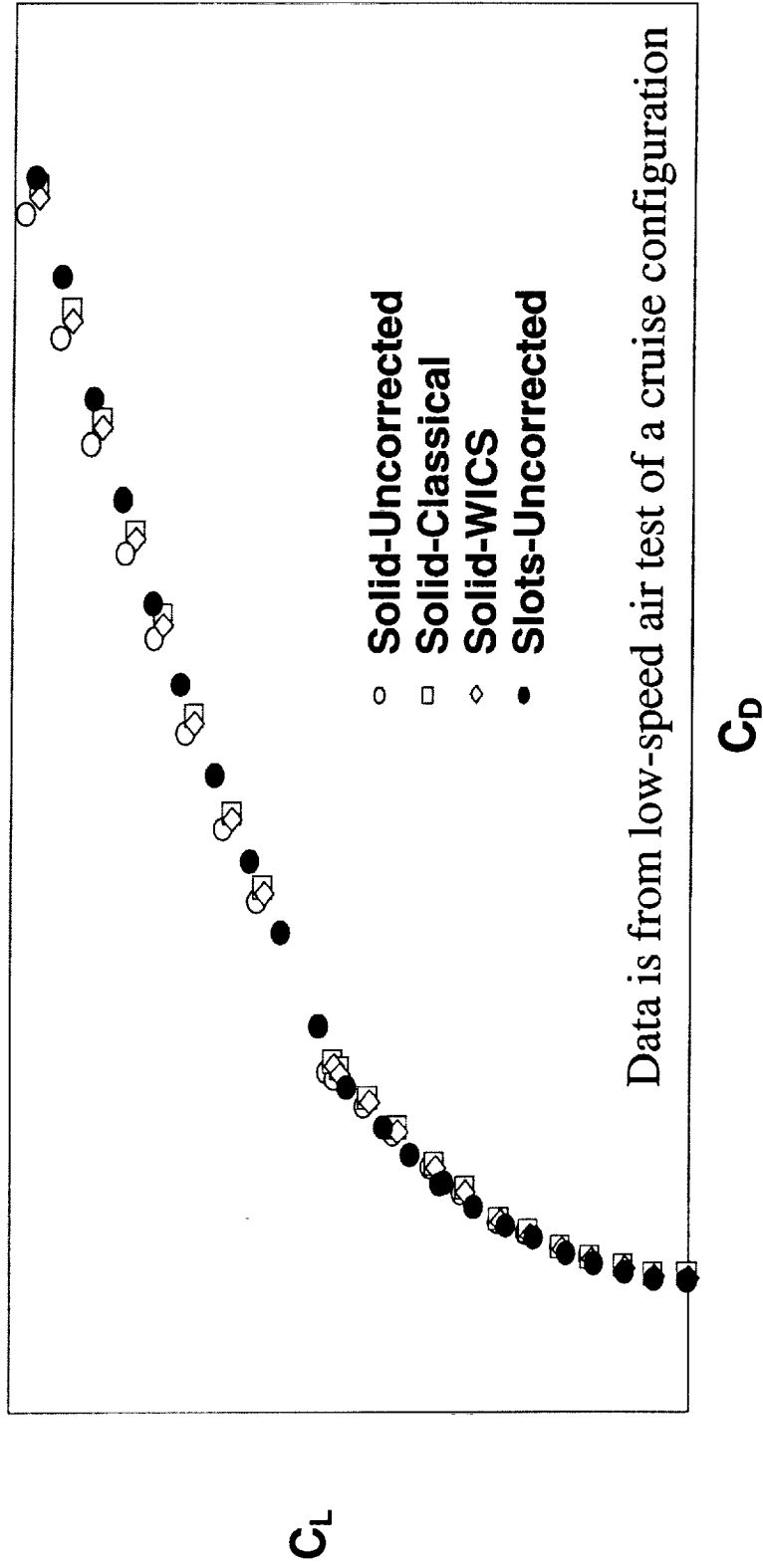


Figure 23 – Wall Interference Corrections, Drag